

# DESIGN AND SIMULATION OF A MINIATURE MOBILE PARTS FEEDER

Arthur E. Quaid  
Ralph L. Hollis

**Abstract** In this work, a miniature mobile vibratory parts feeder is presented. This feeder is designed to reorient, singulate, and position parts by exploiting the horizontal vibration capabilities of a recently developed closed-loop planar motor. The actuators used for generating the vibrations are also capable of large planar motions, allowing the feeder to present parts to multiple overhead robots. It is designed with a minimum of part-specific features, allowing different parts to be fed with only software changes. The basic feed principle is presented and demonstrated experimentally. Although a complete prototype has not yet been fabricated, a model for the motion of parts on the complete feeder is derived and simulation results are presented that indicate successful operation.

## 1 INTRODUCTION

One approach to distributed manipulation is the use of a *single* rigid body to simultaneously manipulate *multiple* parts. The manipulation occurs in multiple locations over the surface of the body, enabling efficient parallel and/or pipelined operation while requiring only a single set of actuators—those needed for moving the body itself. The problem becomes finding a shape and motion for the body so that multiple parts can be manipulated in a useful manner. A related practical problem is the design of the actuation system to realize the desired body motions.

Many have considered combining relatively simple body shapes with vibratory motions, as depicted in Figure 1. Traditional vibratory feeders (a) use inclined vibrations to move parts along a feed track or up a spiral track on the inside of a bowl (Boothroyd et al., 1982). Traps or gates are often placed along the feed path to filter out incorrectly oriented parts. Rotational vibrations (b) of a plate (Böhringer et al., 1995)

## DISTRIBUTED MANIPULATION

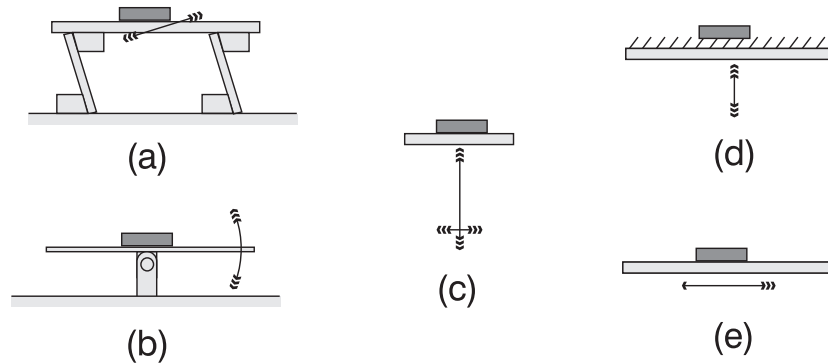


Figure 1 Researchers have explored a variety of distributed manipulation techniques using oscillating plates.

have also been used to orient and localize parts. A bouncing strategy (c) where fast vertical motion of a plate are combined with transverse motion during part impacts has been explored for parallel part reorientation (Singer and Seering, 1987; Swanson et al., 1995). The Dyna-Glide system (d) combines vertical vibrations with a carpet of inclined fibers (Hollington, 1995). Sections of carpets with different directions of inclination can be used over an area to create a desired feed path for parts. It has also been shown (Reznik and Canny, 1998a) that horizontal vibrations of a horizontal plate (e) can be used to move parts in the plane. Surprisingly, this technique was extended (Reznik and Canny, 1998b) to independently control the feed directions of multiple parts sitting on the same horizontal plate.

It is important to specify the purpose of a distributed manipulation system, which may include repositioning, singulating, reorienting, sorting, or even assembling parts. This chapter is concerned with the bulk parts feeding problem: starting with a pile of parts, singulate, position, and orient them for presentation to an assembly device. Of course, parts feeding is of critical importance in automated assembly, and has received much attention. Successful commercial bulk feeders include vibratory feeder bowls (Boothroyd et al., 1982), the Adept FlexFeeder (Arban, 1995; Gudmundsson and Goldberg, 1997), and the Sony APOS system (Krishnaswamy et al., 1996). It is interesting to note that these systems have in common a recirculation path, reorientation facility, and sorting capability. They provide mechanisms for some of the parts to assume the desired orientations, and allow the rest of the parts to be recirculated. Ensuring the parts are in the proper orientation may be done by mechanical means, such as bowl feeder gates or the APOS tray

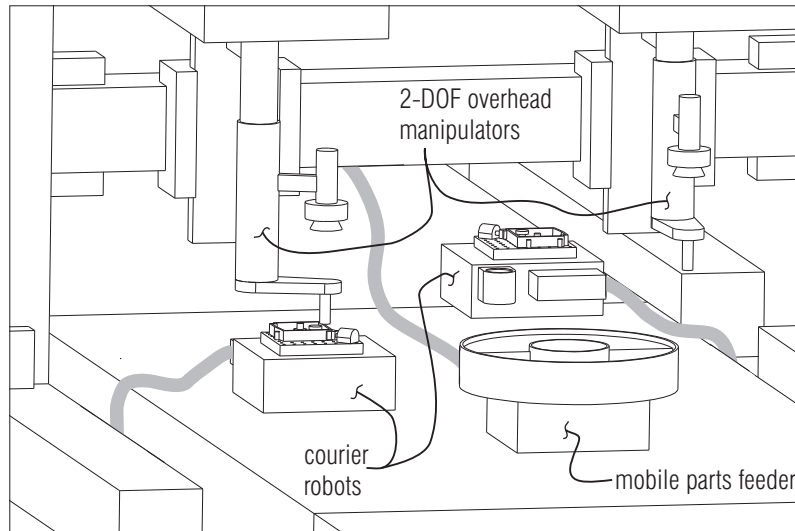


Figure 2 A miniature mobile parts feeder in a minifactory setting: a single feeder supplies parts to multiple low-DOF overhead manipulators.

detents, or through sensing, as in the Adept FlexFeeder vision system. A major advantage of these systems is that every part does not have to be correctly oriented in its first trip through the feeder. With many chances to orient a part, simpler orientation mechanisms can be used without sacrificing robustness.

The remainder of this chapter presents the operating principles and simulation results of a novel bulk parts feeder. This feeder, introduced earlier (Quaid, 1998), is built upon recently developed closed-loop planar motor technology (Butler et al., 1998; Quaid and Hollis, 1998) and seeks to provide a recirculatory feed path in a compact space. A significant novelty is the feeder's mobility, allowing it to supply multiple overhead robots with parts, even if their workspaces do not overlap. The following sub-section provides an application to demonstrate how this mobility can be useful and also presents the basic concept for the feeder.

## 1.1 APPLICATION EXAMPLE

Our particular interest in bulk parts feeding is for use in the *minifactory* (Hollis and Quaid, 1995; Rizzi et al., 1997), an automated assembly system that uses small modular robotic components to reduce design, deployment, and changeover times. This system, depicted in Figure 2, physically consists of a series of tabletop platen tiles connected together

## DISTRIBUTED MANIPULATION

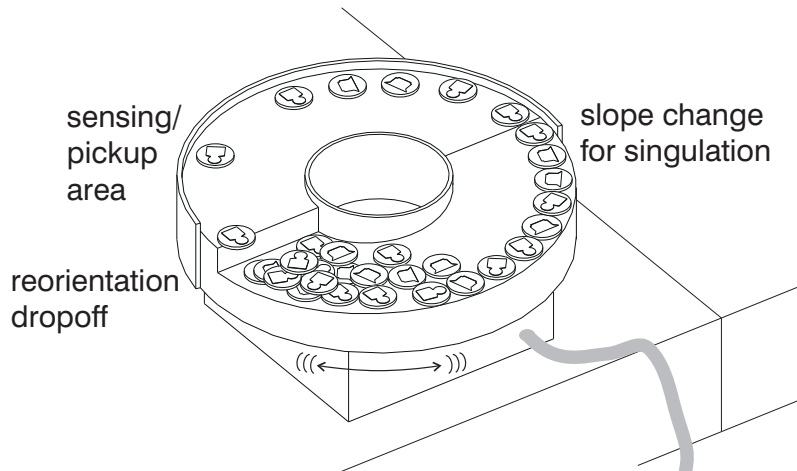


Figure 3 A miniature mobile parts feeder, consisting of a partially sloped annular feed tray (outside edge partially omitted for illustrative purposes) mounted on a planar robot.

to form an extended workspace for *courier* robots. The courier robots have a novel position sensor (Butler et al., 1998) integrated into a planar (Sawyer) motor (Hinds and Nocito, 1974; Pelta, 1987), enabling high-precision closed-loop control. The couriers have a single moving part, ride on air bearings, and can translate large distances along the platen surface (limited only by the length of a tether) and rotate in the plane by a few degrees. Overhead devices such as simple 2-DOF ( $z, \theta$ ) manipulators, glue dispensers, laser welders, etc. are mounted on fixed bridges above the platens. The couriers move product sub-assemblies from one overhead device to another, cooperating with the overhead devices to perform 4-DOF assembly operations.

The overhead manipulators do not have large workspaces, so parts *must* be fed close to the assembly locations. In this context, it is very useful to have a mobile parts feeder that can move under the manipulator with an oriented part, allow the manipulator to pick it up, and then move out of the way.

The proposed mobile parts feeder is depicted in Figure 3. Physically, it consists of a special feed tray rigidly attached to a planar motor. The tray has an annular feed path for parts, with a sloped *ramp* section, and a flat *plateau* section. The motor performs a rotational vibration, resulting in a counter-clockwise motion of the parts. When bulk parts are loaded at the bottom of the ramp, parts slowly climb the ramp, but only near the outside edge, resulting in a single-file line. Once in the

plateau section, the parts speed up and spread out. They continue to move around the plateau, where an overhead vision system can be used to identify parts in the correct orientation.<sup>1</sup> Incorrectly oriented parts are reoriented as they pass over the dropoff and return to the pile of bulk parts. The next section discusses the details of using horizontal vibrations to move parts. Section 3 describes how ramps can be used for singulation. The complete feeder design is then described and simulated in Section 4.

## 2 MOVING PARTS WITH HORIZONTAL VIBRATIONS

In this section, the basic technique for generating part motion is presented. A model is derived and experimental results are presented. As this feeding technique is related to that used by other researchers (Reznik and Canny, 1998a), differences between the approaches are highlighted.

### 2.1 STICK-SLIP WAVEFORM

There is a common magician’s trick where a tablecloth is removed from under a table setting by quickly jerking the cloth. This trick demonstrates how planar motion can cause relative motion between two objects, and inspired our exploration of the application of closed-loop planar motors to parts feeding.

Using a flat plate for the feed tray, motion of parts relative to the tray is achieved by accelerating the feeder rapidly in one direction such that the part slips on the tray, followed by a return to the original position with accelerations slow enough that the part “sticks” to the tray. A periodic waveform with such a *stick-slip* nature is shown in Figure 4.

This waveform is defined as:

$$a(t) = \begin{cases} a_{min} & 0 \leq t \leq t_1 \\ -a_{max} & t_1 < t \leq T - t_1 \\ a_{min} & T - t_1 < t \leq T, \end{cases} \quad (1)$$

$$v(t) = \begin{cases} a_{min}t & 0 \leq t \leq t_1 \\ a_{min}t_1 - a_{max}(t - t_1) & t_1 < t \leq T - t_1 \\ a_{min}(t - T) & T - t_1 < t \leq T, \end{cases} \quad (2)$$

where  $t$  is the time within the current cycle. The acceleration switch time  $t_1$  is computed as:

$$t_1 = \frac{a_{max}}{a_{min} + a_{max}} \frac{T}{2}, \quad (3)$$

so that  $x(T) - x(0) = \int_0^T v(t) dt = 0$ , and the feeder has no net motion.

DISTRIBUTED MANIPULATION

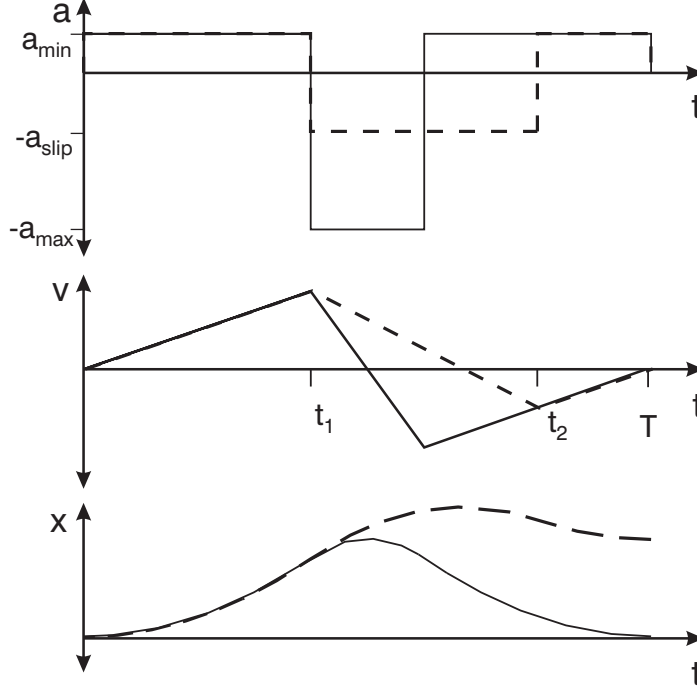


Figure 4 Planar vibratory feeding: at each cycle, the part (dashed trace) moves forward but the tray (solid trace) returns to the original position.

The remaining parameters of the waveform to be chosen are the period  $T$ , the acceleration during the slip phase  $a_{max}$ , and the acceleration during the stick phase  $a_{min}$ . The choice of  $T$  should keep the fundamental frequency of the waveform low enough to be in the dynamic capability of the robot, but high enough to limit the velocities and displacements required of the feeder. Assuming a Coulomb friction model, slipping and sticking will occur properly if  $a_{max}$  and  $a_{min}$  are chosen to meet the constraints  $a_{max} > \mu g$  and  $a_{min} < \mu g$ , where  $g$  is the gravitational acceleration and  $\mu$  is the coefficient of friction between the part and feed tray.

Assuming the part is sticking to the tray at the start of the waveform and its motion is restricted to the direction of tray motion (i.e. no rolling or transverse motion), the part will move as:

$$a_p(t) = \begin{cases} a_{min} & 0 \leq t \leq t_1 \\ -\mu g & t_1 < t \leq t_2 \\ a_{min} & t_2 < t \leq T, \end{cases} \quad (4)$$

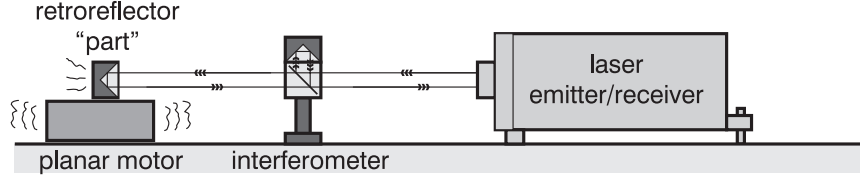


Figure 5 Experimental setup for verifying feed operation: a laser interferometer measures the position of a retroreflector “part”, while the integral planar motor sensor measures the motor position relative to the platen.

$$v_p(t) = \begin{cases} a_{min}t & 0 \leq t \leq t_1 \\ a_{min}t_1 - \mu g(t - t_1) & t_1 < t \leq t_2 \\ a_{min}(t - T) & t_2 < t \leq T. \end{cases} \quad (5)$$

The part catches up to the tray at time

$$t_2 = t_1 + \frac{a_{min}T}{\mu g + a_{min}}, \quad (6)$$

and the average part velocity over one waveform,  $\bar{v}_p$ , is computed as:

$$\bar{v}_p = \frac{Ta_{min}}{2} \left( \frac{-1}{1 + \frac{a_{min}T}{\mu g}} + \frac{1}{1 + \frac{a_{min}}{a_{max}}} \right). \quad (7)$$

To verify the feeding principle, the waveform of Eqs. 1 and 2 was used as the input to one axis of a 3-DOF PD planar motor controller. Parts such as coins, rubber grommets, and plastic pieces with varying friction coefficients were placed on a flat feed tray attached to the motor. Although it was possible to find waveforms that would feed the parts well, not all theoretically acceptable waveforms worked. To investigate further, a stainless steel block containing a glass cube corner was used as the “part,” whose position relative to the stationary platen could be measured using a laser interferometer, as shown in Figure 5. The motor’s position relative to the platen was measured by the integral planar motor sensor. Both position measurements were sufficiently precise and at a high enough bandwidth that simply differencing consecutive measurements provided accurate estimates of the motor and part velocities.

Waveforms that worked well appeared as in Figure 6, with the motor tracking the commanded velocity fairly well. The part velocity deviates from the motor velocity during the slip phase and tracks it closely during the stick phase, as expected. Given the feeder waveform parameters and estimated friction coefficient,  $\bar{v}_p$  is computed using Eq. 7 as 11.8 mm/s.

## DISTRIBUTED MANIPULATION

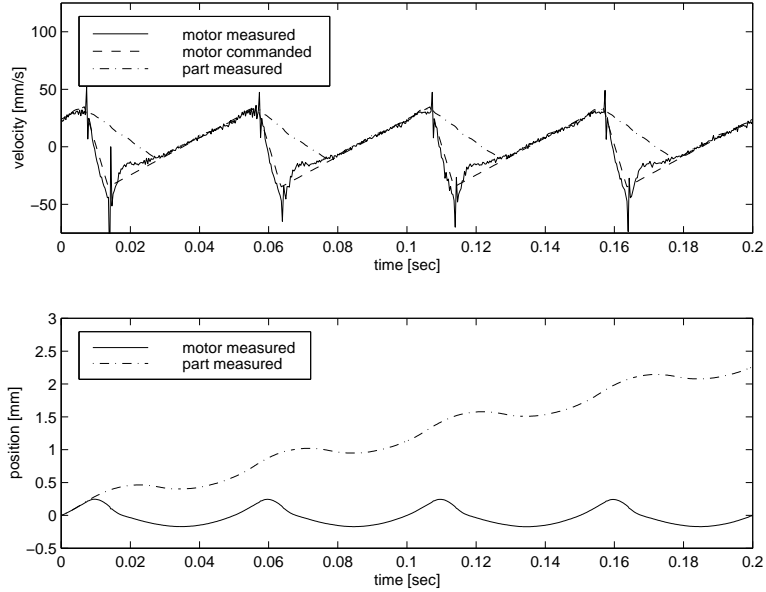


Figure 6 Experimental measurements of feeder and part motion using a stick-slip waveform with  $T = 0.05$  s,  $a_{min} = 1.6$  m/s<sup>2</sup>,  $a_{max} = 10.1$  m/s<sup>2</sup>. The part is stainless steel and the tray is aluminum; based on the part motion during the slip phase, the coefficient of friction appears to be approximately 0.2.

In the experiment, the part traveled about 2.48 mm over 0.2 s, for an average velocity of 12.4 mm/s, in close agreement with the predicted value.

In waveforms that did not work well, the motor velocity had large deviations from the commanded velocity. Improved calibration of the motor sensors and actuators, and development of controllers with improved tracking abilities will reduce the need for careful tuning of the waveform parameters.

## 2.2 COULOMB PUMP WAVEFORM

A *Coulomb pump* waveform has also been used (Reznik and Canny, 1998a; Reznik and Canny, 1998b) to achieve part motion in the plane. This waveform is given by:

$$a_t(t) = \begin{cases} a_{max} & 0 \leq t < t_1 \\ 0 & t_1 \leq t < t_2 \\ -a_{max} & t_2 \leq t < T, \end{cases} \quad (8)$$

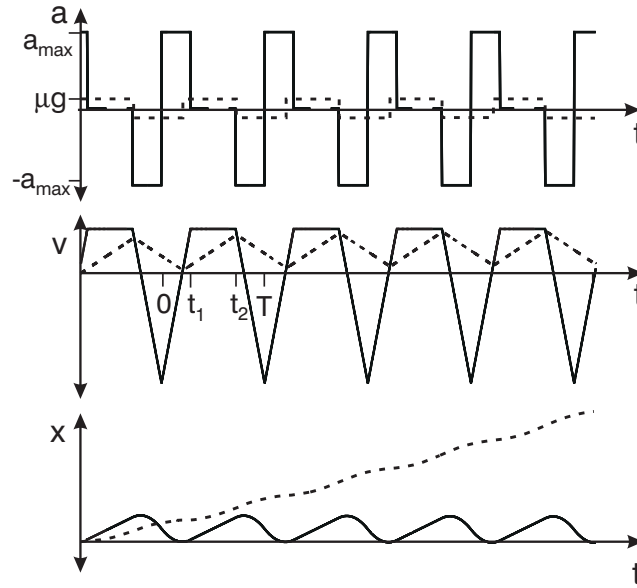


Figure 7 The Coulomb pump waveform can achieve higher part velocities over multiple cycles.

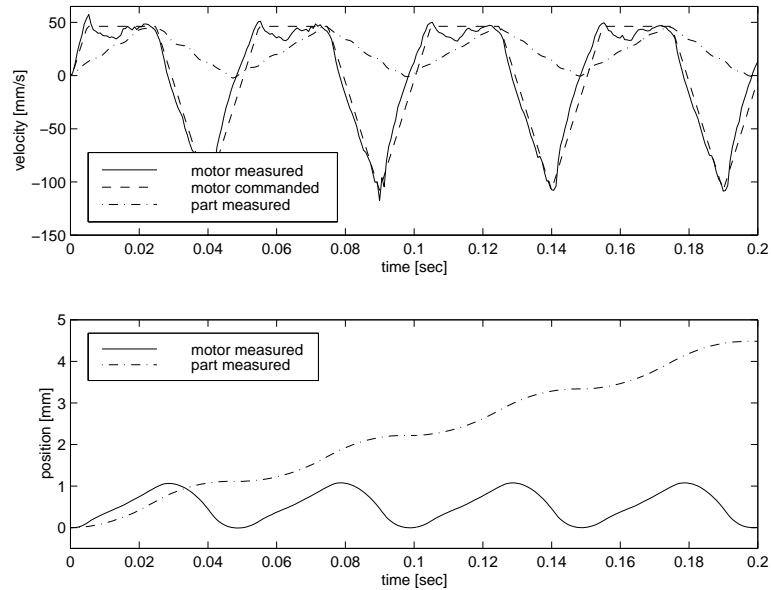


Figure 8 Experimental measurements of feeder and part motion using a Coulomb pump waveform with  $T = 0.05$  s,  $a_{max} = 10.3$  m/s<sup>2</sup>, and  $z = 0.37$ .

DISTRIBUTED MANIPULATION

$$v_t(t) = \begin{cases} a_{max} \left[ \frac{T}{4}(z^2 - 1) + t \right] & 0 \leq t < t_1 \\ a_{max} \frac{T}{4}(z - 1)^2 & t_1 \leq t < t_2 \\ a_{max} \left[ \frac{T}{4}(z^2 + 3) - t \right] & t_2 \leq t < T, \end{cases} \quad (9)$$

where  $t_1 = (1 - z)T/2$ ,  $t_2 = (1 + z)T/2$ , and  $z$  is a parameter controlling the fraction of a cycle used by the constant velocity portion of the waveform.

As shown in Figure 7, the part motion changes from cycle to cycle, with each cycle “pumping up” the velocity via the Coulomb friction forces. The part velocity is now best characterized by the *equilibrium velocity*, which is the value that the average waveform velocity eventually reaches, given by (Reznik and Canny, 1998a):

$$v_{eq} = a_{max} T \frac{z^2}{4}. \quad (10)$$

The Coulomb pump waveform was also implemented on one axis of the planar motor. Once again, the main problem was in finding a waveform that the motor followed reasonably well. One example is shown in Figure 8. Applying Eq. 10, the computed equilibrium velocity is 17.6 mm/s, while the observed velocity in Figure 8 is 4.5 mm/0.2 s, or 22.5 mm/s, a fairly close match.

The examples shown in Figure 6 and Figure 8 (which both use the same part and similar waveform frequencies and maximum accelerations) show that the Coulomb pump waveform has a higher part velocity than the stick-slip waveform, but requires larger velocity and translations from the feeder. The larger forward accelerations of this waveform also appear to cause problems for sloped feed trays, as discussed in the following section.

### 3 SINGULATING PARTS WITH RAMPS

While the above waveforms result in part motion, nearby parts will tend to move as a group. It is often useful to also singulate parts so that a vision system or manipulator does not need to deal with nested or adjacent parts. One technique for singulation is to somehow vary the feed rate of the parts based on their position. In particular, if the feed rate increases as the parts move from one region to another, the parts will tend to spread out. This technique is used in the dual conveyors of the Adept FlexFeeder (Gudmundsson and Goldberg, 1997), schematically shown in the top half of Figure 9, where one conveyor drops parts onto a faster conveyor. To achieve a similar effect for the proposed feeder,

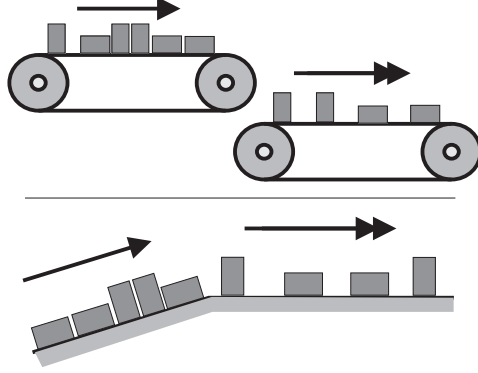


Figure 9 A change of feed velocity based on part position can singulate parts in the direction of motion. This technique can be implemented with conveyors (above) or a sloped feed tray (below).

a sloped section may be added to the feeder tray. Assuming that parts will climb up the ramp, but at a slower rate than if they were on a flat surface, the parts on the flat plateau region at the top of the ramp will be singulated relative to the parts on the ramp section, as depicted in the bottom half of Figure 9. A model for parts motion on ramps is derived in this section that supports this conclusion.

For this case, the part dynamics are given by inspection of the free-body diagram in Figure 10:

$$m\ddot{y}_p = f_f - mg \sin(\varphi) \quad (11)$$

$$m\ddot{z}_p = f_N - mg \cos(\varphi), \quad (12)$$

where  $\ddot{y}_p$  and  $\ddot{z}_p$  are the part accelerations in the  $j$  and  $k$  directions defined in Figure 10. Assuming a Coulomb friction model and sliding contact between the part and ramp, there are two additional constraints:

$$f_f = -\mu f_N, \quad \text{and} \quad (13)$$

$$\ddot{z}_p = -\ddot{y}_t \sin(\varphi), \quad (14)$$

where  $\ddot{y}_t$  is the horizontal tray acceleration.

Solving the above equations for  $f_N$ ,  $\ddot{y}_p$ , and  $\ddot{z}_p$  gives:

$$f_N = mg \cos(\varphi) - m\ddot{y}_t \sin(\varphi) \quad (15)$$

$$\ddot{y}_p = -g \sin(\varphi) - \mu g \cos(\varphi) + \mu \ddot{y}_t \sin(\varphi) \quad (16)$$

$$\ddot{z}_p = -\ddot{y}_t \sin(\varphi). \quad (17)$$

Note that  $\ddot{y}_p$ , the part acceleration, is now a function of the tray acceleration, which changes during the slip phase, complicating the part

DISTRIBUTED MANIPULATION

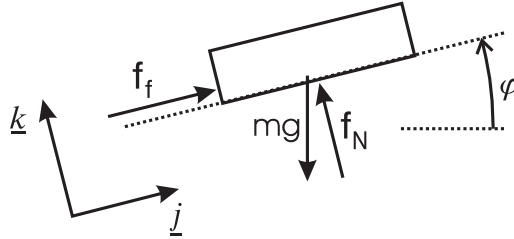


Figure 10 Free body diagram for part on ramp

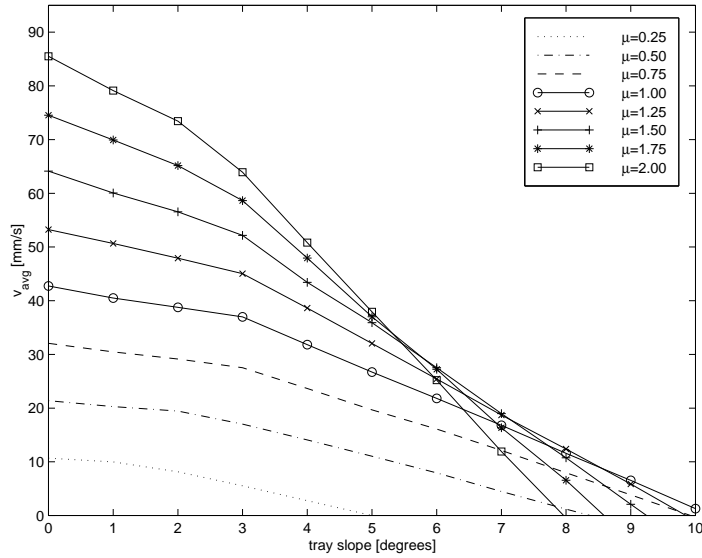


Figure 11 Feed rates as a function of tray slope and coefficient of friction for stick-slip waveform, with  $a_{max} = 4\mu g$ ,  $a_{min} = 0.9\mu g$ , and  $T = 1/30$  s. Parts feed faster on flat surfaces than up ramps.

motion. For this reason, an analytic solution of the part motion is less informative than for the flat tray case, and the dynamic equations are instead used to simulate the part motion.

The part motion was simulated for a range of friction coefficients and ramp angles, with results shown in Figure 11. It is interesting to note that for some of the cases represented in this plot, the stick assumption does not hold, but parts still move forward. More importantly, the feed rate for parts on a ramp is smaller than for parts on a flat surface,

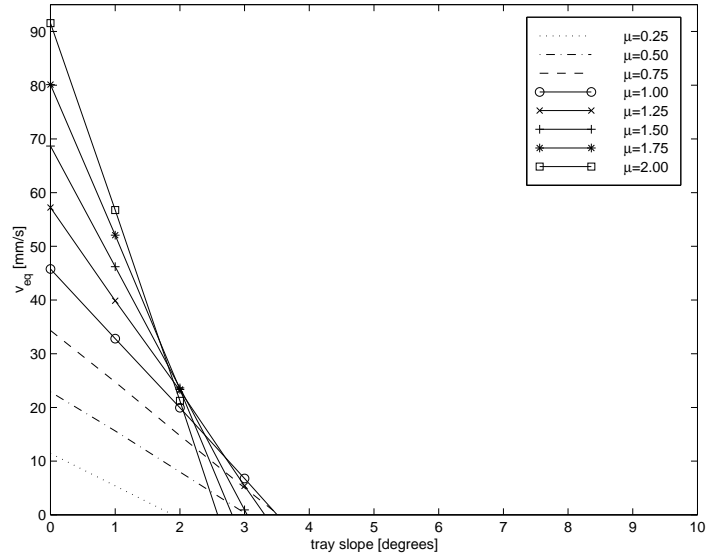


Figure 12 Feed rates as a function of tray slope and coefficient of friction for Coulomb pump waveform, with  $a_{max} = 4\mu g$  and  $T = 1/30$  s.

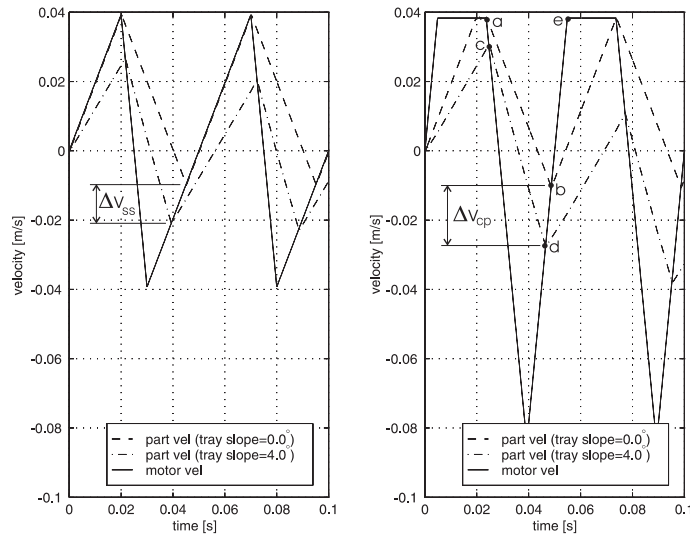


Figure 13 Part waveforms change based on the slope of the feed tray for both the stick-slip (left) and Coulomb pump (right) waveforms.

suggesting that a ramp will be effective for singulation. The left half of Figure 13 shows an example of how the motion of a part on a sloped feed tray compares with that of a part on a flat feed tray.

Simulations of the Coulomb pump waveform for the sloped feed tray were also performed, with results shown in Figure 12. Here, the part velocity dropped off faster with increasing slope than for the stick-slip waveform. Note that the part velocity drops below zero at about  $3^\circ$ , limiting this waveform to gradual slopes. The reason for this effect is difficult to pinpoint, but appears to be related to the larger positive accelerations of the tray. Referring to the right half of Figure 13, when the slope of the part velocity increases from  $\overline{ab}$  to  $\overline{cd}$ , the change in the minimum part velocity,  $\Delta v_{cp}$ , will be greater if the slope of  $\overline{de}$  is larger. In particular, note that  $\Delta v_{cp} > \Delta v_{ss}$ , indicating that the slope change has a larger effect on the Coulomb pump waveform. Although such a change is useful for singulation, in this case it is too extreme and will limit the feasible ramp angles too severely.

#### 4 A MINIATURE MOBILE PARTS FEEDER

In the complete feeder design (Figure 3), the above motion and singulation techniques are combined with a parts recirculation strategy, chosen for the reasons cited in Section 1. The feeder has an annular feed path so that a single rotational vibration waveform of the feeder will suffice to keep the parts flowing around the loop. A ramp is used, as discussed above, to singulate parts along the direction of feeding. Two effects were expected to provide singulation radially across the feed path. First, the parts were expected to move locally along tangents, which would tend to make them collect towards the outer wall of the feed tray. In addition, the ramp section does not have a constant slope, but gets steeper with decreasing radius. If the waveform is selected carefully, it could be possible to cause parts to slide back down the ramp for small radii, but still climb at larger radii. This technique would allow for a variable-width feeding region at the outer wall of the feed tray. Simulation results below examine these effects.

Once singulated and in the plateau region, an overhead vision system can be used to detect parts in the correct orientation. The feeder can then move<sup>2</sup> to deliver the parts to an overhead manipulator for assembly.

Incorrectly oriented parts rejected by the vision system continue around the feed path and pass over the dropoff (a nice side-effect of the ramp section). The dropoff allows the feeder to reorient parts out of the plane, despite the strictly planar motion of the feeder. Depending on the part

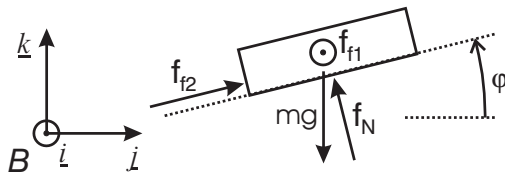


Figure 14 Local free body diagram for a part on an annular tray. ( $\odot$  denotes a vector pointing out of the page.)

materials, part size and shape, and dropoff height, the part might always just flip over or might assume a more random orientation change.

Although the proposed feeder physically resembles a vibratory bowl feeder, it is important to note the major differences. First, the proposed feeder design is intended for use where feeder bowls custom-designed for parts would be impractical because of re-use requirements or long lead times, and where required feed rates are modest. Conceptually, the feeder operation actually resembles the Adept FlexFeeder (with the ramp singulation replacing the double conveyors and both using vision for parts selection) more than a bowl feeder. Second, the use of planar motor technology for generation of vibrations allows the feeder to be compact and mobile, permitting it to deliver parts directly to the assembly location, which is especially important for the minifactory application.

#### 4.1 DYNAMIC MODEL

To simulate the motion of a part on the above tray, a dynamic model is first derived. The part is assumed to be a point mass that stays in contact with the feed tray, and a Coulomb friction model is assumed. A free-body diagram of the part on the ramped section of the tray is shown in Figure 14. Coordinate frame  $B$  is an inertial (not accelerating) reference frame aligned with the part *at this particular instant in time*.<sup>3</sup> The dynamics of both a sticking case and slipping case must be considered. The dynamics problem is to determine the acceleration of the part along the tray given the part and tray positions and velocities.

By inspection of the free-body diagram, the part dynamics are given by:

$$\ddot{x} = f_{f1}/m, \quad (18)$$

$$\ddot{y} = f_{f2} \cos(\varphi)/m - f_N \sin(\varphi)/m, \quad (19)$$

$$\ddot{z} = f_{f2} \sin(\varphi)/m + f_N \cos(\varphi)/m - g, \quad (20)$$

## DISTRIBUTED MANIPULATION

where  $f_{f1,2}$ ,  $f_N$ ,  $g$ , and  $\varphi$  are defined in Figure 14.

For the slipping case, Coulomb's law gives:

$$\mathbf{f}_f = \begin{bmatrix} f_{f1} \\ f_{f2} \cos(\varphi) \\ f_{f2} \sin(\varphi) \end{bmatrix} = \mu f_N \frac{\mathbf{v}_p - \mathbf{v}_t}{\|\mathbf{v}_p - \mathbf{v}_t\|}, \quad (21)$$

where  $\mathbf{v}_p$  is the part velocity and  $\mathbf{v}_t$  is the local tray velocity, both expressed in coordinate frame  $B$ .

Assuming the part stays on the surface of the feed tray, there is an additional kinematic constraint on the part acceleration:

$$\ddot{z} = \tan(\varphi)(\ddot{y} - 2\dot{r}\dot{\theta} - r\ddot{\theta}_t), \quad (22)$$

where  $r$  and  $\theta$  give the part position in polar coordinates relative to the center of the feeder, and  $\theta_t$  is the rotation angle of the feeder.

To solve for  $f_N$ , Eqs. 19 and 20 are substituted into Eq. 22, yielding:

$$f_N = mg \cos(\varphi) - 2m \sin(\varphi) \dot{r}\dot{\theta} - m\ddot{\theta}_t \sin(\varphi). \quad (23)$$

This result for  $f_N$  can then be substituted into Eq. 21 to get  $f_{f1,2}$ , and Eqs. 18-20 to compute the part acceleration for the slipping case at a given instant in time. Because coordinate frame  $B$  is only valid at an instant in time, the acceleration vector must be transformed to a coordinate frame fixed to the workspace before integration.

For the sticking case, the part is fixed relative to the feed tray, and the part accelerations are given based on the tray motion and part position:

$$\ddot{x} = -r\dot{\theta}_t^2 \quad (24)$$

$$\ddot{y} = r\ddot{\theta}_t \quad (25)$$

$$\ddot{z} = 0, \quad (26)$$

To check whether the friction forces are sufficient to keep the part stuck to the feed tray, these acceleration values are substituted into Eqs. 18-20, which can be solved for  $f_N$  and  $f_{f1,2}$ :

$$f_N = -mr\ddot{\theta}_t \sin(\varphi) + mg \cos(\varphi) \quad (27)$$

$$f_{f1} = -mr\dot{\theta}_t^2 \quad (28)$$

$$f_{f2} = mr\ddot{\theta}_t \cos(\varphi) - mg \sin(\varphi). \quad (29)$$

Both the sticking and sliding equations are evaluated every simulation iteration. The sticking mode results are used if  $\|[f_{f1} \ f_{f2}]^T\| < \mu f_N$  (which indicates that the friction forces are sufficient to maintain sticking), and the relative velocity  $\|\mathbf{v}_p - \mathbf{v}_t\|$  is below some threshold. Otherwise, the sliding mode results are used. For both cases, the sign of  $f_N$  is checked to be sure the part does not leave the tray surface.

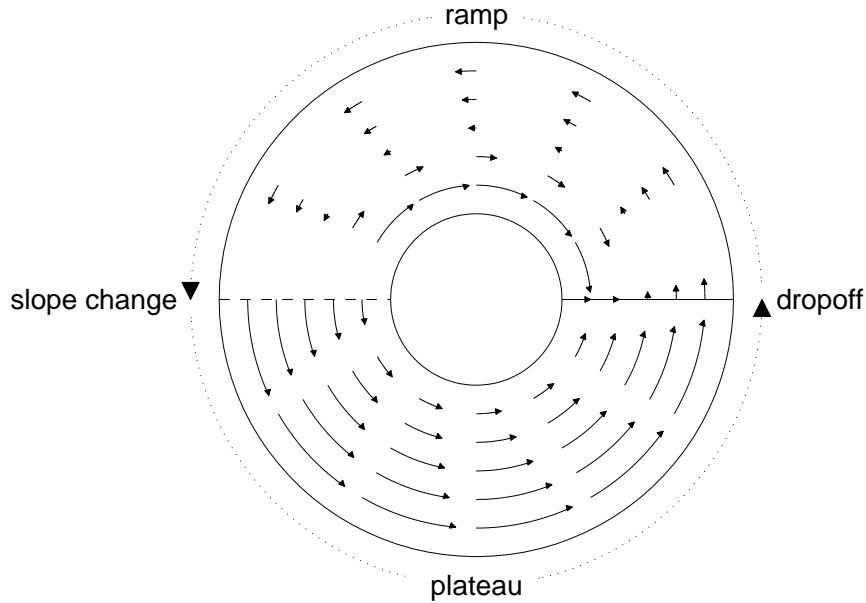


Figure 15 Simulation results show parts climbing the curved ramp, and singulation occurring in the radial and circumferential directions.

## 4.2 SIMULATION RESULTS

Simulations were performed for a feeder with an outer radius of 90 mm, an inner radius of 30 mm, and a  $180^\circ$  ramp with a total height change of 20 mm. The part mass is chosen as 20 g, with a coefficient of friction between the part and tray of  $\mu = 0.2$ . The tray is set to follow a rotational stick-slip waveform, with parameters  $T = 1/30$  s,  $a_{min} = 9.0\mu g$   $\text{rad/s}^2$ , and  $a_{max} = 66.7\mu g$   $\text{rad/s}^2$ . The initial position of the part is set to one of a polar array of positions on the tray, with zero initial velocity. For each starting position, the part motion is simulated for five seconds while recording the sequence of part positions.

Results for each part starting position are shown in Figure 15. Note that parts only feed up the ramp if they are close to the outer radius of the feeder, with retrograde motion of parts near the center. This feed pattern should cause the parts to form a single-file line, effectively singulating them in the radial direction. The part velocity on the plateau section is much faster than that on the ramp, suggesting that singulation along the direction of motion should also work well. It is surprising that the parts move along nearly perfect arcs, instead of veering off in more of a tangent direction. This effect can be understood by noting that the

## *DISTRIBUTED MANIPULATION*

parts move in a series of small incremental steps that closely approximate a circle. Also, sticking resets the radial velocity of the part to zero every cycle. A depiction of the parts flow in the feeder loosely based on the these simulation results is shown in Figure 3.

A simulation of the feeder using the Coulomb pump waveform was also attempted. However, it was difficult to get the parts to climb the ramp except for very gradual slopes, with 5 mm or less rise over the 180° ramp. This result was not surprising given this waveform's strong sensitivity to slope, as noted in Section 3.

## **5 SUMMARY**

The design, operation, and simulation of a novel miniature mobile parts feeder was presented. Experimental results of the basic feed principle confirmed the feed model. Simulation results indicate a promising ability to feed and singulate parts within a compact recirculating device.

Open problems include choosing the waveform parameters given a particular feed tray and part, and designing a feed tray for a family of parts given the limitations of the planar motor actuators. In addition, waveforms other than the stick-slip or Coulomb pump can be considered. A hybrid waveform that combines their advantages or the formulation of an optimal waveform would improve performance.

There are a number of potential limitations of this feeder. Parts must be stable enough in their pickup orientation to survive the trip up the ramp and the vibrations without falling over. Parts that tend to nest will probably not be singulated properly. Parts may become stuck on the transition between the ramp and plateau, even if it is rounded. Feed rates may be too slow to be useful in a real automated assembly system. However, the results so far are encouraging enough that we intend to build a prototype parts feeder of this type. Fabrication techniques for the feed tray are being considered, and improved calibration and control of the planar motor to allow for more precise tracking of the commanded waveforms is being investigated.

## **Acknowledgments**

The authors wish to thank Matt Mason for helpful discussions and especially for suggesting the use of ramps for singulation purposes. This work is supported in part by NSF grants DMI-9523156 and CDA-9503992. Quaid is supported by a Lucent Technologies Foundation Fellowship.

## Notes

1. It is also possible to place indentations, fences, etc. in the plateau region to separate parts in the correct orientation without the use of vision. However, unless a removable insert contains all the part specific features, the feeder's flexibility will be somewhat compromised.
2. Of course, it must move with small enough accelerations that the parts don't slide relative to the feed tray.
3. In the simulation, each time step uses a different frame  $B$ .

## References

- Arban, A. (1995). Adept parts feeder. *Assembly Automation*, 15(3):36–37.
- Böhringer, K.-F., Bhatt, V., and Goldberg, K. Y. (1995). Sensorless manipulation using transverse vibrations of a plate. In *Proc. IEEE Int'l Conf. on Robotics and Automation*, pages 1989–1996.
- Boothroyd, G., Poli, C., and Murch, L. E. (1982). *Vibratory Bowl Feeders*, chapter 3, pages 27–49. Marcel Dekker, Inc.
- Butler, Z. J., Rizzi, A. A., and Hollis, R. L. (1998). Integrated precision 3-DOF position sensor for planar linear motors. In *Proc. IEEE Int'l Conf. on Robotics and Automation*.
- Gudmundsson, D. and Goldberg, K. (1997). Tuning robotic part feeder parameters to maximize throughput. In *Proc. IEEE Int'l Conf. on Robotics and Automation*, pages 2440–2445.
- Hinds, W. E. and Nocito, B. (1974). 15: The Sawyer linear motor. In Kuo, B., editor, *Theory and Application of Step Motors*, pages 327–340. St. Paul, West Publishing Co.
- Hollingham, J. (1995). Sweeping it over the carpet. *Assembly Automation*, 15(3):29–30.
- Hollis, R. L. and Quaid, A. (1995). An architecture for agile assembly. In *American Society of Precision Engineering 10th Annual Meeting, Austin, Texas*, pages 372–375.
- Krishnaswamy, J., Jakiela, M. J., and Whitney, D. E. (1996). Mechanics of vibration-assisted entrapment with application to design. In *Proc. IEEE Int'l Conf. on Robotics and Automation*, pages 838–845.
- Pelta, E. R. (1987). Two-axis Sawyer motor for motion systems. *IEEE Control Systems magazine*, pages 20–24.
- Quaid, A. E. (1998). A miniature mobile parts feeder: Operating principles and simulation results. Technical Report CMU-RI-TR-98-26, The Robotics Institute, Carnegie Mellon University.
- Quaid, A. E. and Hollis, R. L. (1998). 3-DOF closed-loop control for planar linear motors. In *Proc. IEEE Int'l Conf. on Robotics and Automation*.

*DISTRIBUTED MANIPULATION*

- Reznik, D. and Canny, J. (1998a). The Coulomb pump: a novel parts feeding method using a horizontally-vibrating surface. In *Proc. Int'l Conf. on Intelligent Robots and Systems*, pages 869–874.
- Reznik, D. and Canny, J. (1998b). A flat rigid plate is a universal planar manipulator. In *Proc. Int'l Conf. on Intelligent Robots and Systems*, pages 1471–1477.
- Rizzi, A. A., Gowdy, J., and Hollis, R. L. (1997). Agile assembly architecture: an agent based approach to modular precision assembly systems. In *Proc. IEEE Int'l Conf. on Robotics and Automation*, pages 1511–1516.
- Singer, N. C. and Seering, W. P. (1987). Utilizing dynamic stability to orient parts. *Journal of Applied Mechanics*, 54:961–966.
- Swanson, P., Burridge, R., and Koditschek, D. (1995). Global asymptotic stability of a passive juggler: A parts feeding strategy. In *Proc. IEEE Int'l Conf. on Robotics and Automation*, pages 1983–1988, Nagoya, Japan.